IEEE Access
Multidisciplinary | Rapid Review | Open Access Journal

Received 26 July 2022, accepted 23 September 2022, date of publication 6 October 2022, date of current version 13 October 2022.

Digital Object Identifier 10.1109/ACCESS.2022.3212791

RESEARCH ARTICLE

A Digital Realization of Neuroglial Interaction Model and Its Network Structure

MAHSASADAT SEYEDBARHAGH[1], ARASH AHMADI[2], (Senior Member, IEEE), AND MAJID AHMADI[1], (Life Fellow, IEEE)

[1]Electrical and Computer Engineering Department, University of Windsor, Windsor, ON N9B 3P4, Canada
[2]Electronic Department, Carleton University, Ottawa, ON K1S 5B6, Canada

Corresponding author: Mahsasadat Seyedbarhagh (seyedba@uwindsor.ca)

ABSTRACT Astrocyte cells, the most existing abundant cells in central nervous system, play an essential role in modulating the neuronal activities, information processing, and regulating the synaptic plasticity through calcium (Ca2+) fluctuations of ions hemostasis by using a feedback mechanism. The pathophysiological and hypersynchronous neuronal activity can lead to the epileptic seizures, which is known as one of the neurodegenerative disorders in the field of neuroscience. This paper presents a modified neuron-astrocyte interaction (tripartite synapse) model based on leaky and integrate fire neuron and the astrocyte-synapse models using an area-efficient hardware approach called stochastic computing paradigm. The proposed model is synthesized physically on field-programmable gate array as a proof of concept. The implementation results of the presented model can mimic the bidirectional communication in biological minimal network of pre-postsynaptic and Ca2+-based model for astrocyte with considerably lower hardware cost. The influence of astrocytes on neural network behavioral has been investigated by providing a proper feedback mechanism and considering the role of gap junction coupling and the various coefficients on desynchronizing the impaired synchronization of the coupled neurons.

INDEX TERMS Astrocytes, desynchronization, field programmable gate array (FPGA), neural-glial interaction.

I. INTRODUCTION

Epilepsy is one of the neurological malfunction disorders which occurs due to the unusual patterns of neuronal firing and hypersynchronous neuronal activities. Authors in [1] and [2] have investigated the impact of astrocytes during epilepsy in synchronizing the coupled neurons in network level by proposing different functional modeling. One of the fundamental elements which are involved in the development of enormous neuron motor disorders are astrocytic cells. Astrocytes within central nervous system (CNS) are involved for modulating synaptic plasticity and transmission between neurons through hemostasis and metabolic processes [3].

Recently, neuromorphic VLSI implementation of neural networks has been investigated to discover the implementation of the large-scale Spiking Neural networks [4], [5]. Hardware implementation of various biological models can be achieved using mainly two different platforms. First approach is analog implementation which provides an efficient and low-cost design in terms of occupied area, hardware resources, and power consumption but its development time is longer, its vulnerability to noise is higher, and it is an inflexible approach in comparison to digital platforms. In [6] and [7], analog designs are proposed for the biological models. Alternatively, digital implementation, which has recently become a popular approach to bio-inspired computing which can offer a flexible and reconfigurable design. Digital platforms require a shorter development time in comparison to analog platforms. In this sense, FPGA-based designs can provide a higher level of precision and stability than other types of designs [8].

In this paper, a computationally low-cost hardware based tripartite synapse model according to a neuroglial interaction model has been proposed and implemented on FPGA which

The associate editor coordinating the review of this manuscript and approving it for publication was Gian Domenico Licciardo.

is able to mimic the original behavior of the tripartite synapse model. The main contributions of this paper are listed as follows:

- An efficient digital design for a minimal network using Stochastic Computing technique which can mimic the original architecture of neuron-glial interaction.
- Investigating the influence of astroglia network on controlling the neuronal hyperexcitability during epileptic seizures by stabilizing the asynchrony behavioural between the coupled neurons.
- The proposed design is implemented on both hardware and software and has been compared with the original and other similar designs of hardware tripartite synapse models.

The rest of the paper is organized as follows. Section II discovers the related works. A complete tripartite synapse model which is composed of two neurons, an astrocyte, and the synapse model has been discussed in section III. Section IV discusses the proposed structure. Hardware implementation based on the modified model is presented in Section V. Section VI presents a neuroglial network model. The implementation results are shown in Section VII. This article is concluded in Conclusion section.

II. RELATED WORKS

Many neuropathological disorders such as epileptic seizures [9], Parkinson's disease [10], and sleep-related disturbances [11] are required to be carefully studied in order to discover possible pathways for diagnostic and treatment approaches. In recent years, bidirectional interaction between astrocytic network and neuronal activity have been determined in the area of computational neuroscience. This interaction can be understood in a feedback-based manner to accommodate the intermittent neuronal synchrony.

Different models are proposed for modelling the bidirectional communication for neuron-astrocyte interactions to demonstrate the impact of astrocytes on the dynamics of spiking activity in neural network [12], [13], [14], [15]. In these articles, a mathematical model for neuron-astrocyte interaction system is proposed which can describe the tripartite synapse including pre-postsynaptic neurons, Ca2+ oscillations in astrocyte and synapse model. Calcium elevation in astrocyte can mediate the gliotransmitter release such as gamma aminobutyric acid (GABA), adenosine triphosphate (ATP), glutamate which results neuronal excitability through a feedback mode and can activate postsynaptic neurons at other synaptic terminals. On the other hand, glial cells can communicate with each other via Gap Junctions by transmission of IP3 molecules and Ca2+ waves propagations. Di Garbo and colleagues in [12] proposed a minimal biological neural network for describing the glial-neuron interaction which considered the impact of ATP on modulating neuronal activities. A dressed neuron model by describing the neuron-astrocyte interaction is proposed by Jung and Nadkarni [13]. A mathematical model is proposed for the elements of tripartite synapse in [14] and [15] which can reproduce the dynamical patterns of the biological neuron-astrocyte network.

Several hardware implementations for various biological calcium-based neuron-astrocyte models are proposed on FPGA platforms in [16], [17], [18], [19], and [20]. There are some approaches that can be employed to develop digital neuromorphic circuits. One of these approaches is base-2 method in which nonlinear terms of biologically inspired models can be replaced with base-2 functions and physically implemented using logical shift and add operations on hardware [20], [21]. The next approach is CORDIC (coordinate rotation digital computer) structure which is involved in computing complicated nonlinear functions through simple shift and add operations [16], [22]. This technique can cause the simplicity of the hardware implementation for the biologically plausible models; however, the main drawback associated with CORDIC paradigm is the latency issue. Piece-wise linear approximation method can be used to eliminate the nonlinearity of the biologically plausible models by utilizing several linear segments [17], [23]. In order to elevate the accuracy of the design, the number of linear segments are needed to be increased which can result in escalating the hardware cost. The last method is called stochastic computing (SC) approach which is an efficient hardware-based scheme. This method uses simple digital circuits to perform the arithmetic operations and is proposed initially in 1960s [24]. This architecture can be represented in both bipolar and unipolar formats [25], [33]. The main concept of this probabilistic-based computing approach is to process data by utilizing the digitized probabilistic unary stream. In recent years, SC method has gained greater insight in hardware realization of neural networks and neuromorphic computing studies due to its error-tolerant inherent and the optimized performance in terms of power and occupied area [26]. In [27], authors have proposed a hardware based tripartite synapse including Leaky Integrate-and-Fire (LIF) neuron, synapse, and astrocyte using Stochastic Computing (SC) and the Extended Stochastic Logics (ESLs). ESLs has been introduced as new method for SC for the hardware design of neural network applications [28]. In their work [27], astrocyte model is approximated using piece wise linear approximation method. Recently, a digital design for an optimized SC-based Izhikevich spiking neuron model is presented in [29].

The main predominancy of the proposed model over the recently published SC-based neuroglial model in [27] is that a detailed architecture for astroglial model and the hardware device utilization is discussed within this research study.

III. MATERIAL AND METHOD

A. NEURON MODEL

In this paper, leaky integrate-and-fire (LIF) neuron model with adaptation current which is one of the simplest spiking neuron models has been used to describe the spiking behaviour of the presynaptic and postsynaptic neurons. LIF spiking neuron fires when the membrane voltage becomes greater than threshold level. This model can be described

by the following differential equations, respectively [30] and [43]:

$$\begin{cases} C\frac{dV_{Pre}}{dt} = -g_L\left(V_{Pre} - E_L\right) - I_{Pre} \\ \frac{dw_{Pre}}{dt} = -\frac{1}{\tau}\left(w_{Pre}\right) \end{cases} \quad (1)$$

$$\begin{cases} C\frac{dV_{Post}}{dt} = -g_L\left(V_{Post} - E_L\right) - I_{Post} \\ \frac{dw_{Post}}{dt} = -\frac{1}{\tau}\left(w_{Post}\right) \end{cases} \quad (2)$$

where $C, V_{Pre}, V_{Post}, w_{Pre}, w_{Post}, g_L, E_L$, and τ present the membrane capacitance, membrane potentials and variable of adaptation currents for presynaptic and post synaptic neurons, the conductance of leaky channels, the leak reversal potential, and time constant for adaptation current, respectively. The following listed equations are used to describe the behavior of the presynaptic I_{Pre} and postsynaptic currents I_{Post}:

$$\begin{cases} I_{Pre} = I_{applied} + I_a \\ I_{Post} = I_e + I_{Glu} + I_{ATP} + I_a \\ I_{Glu} = \gamma G_m \\ I_{ATP} = \eta G_a \\ I_e = g_e\left(V - E_e\right) \\ I_a = w\left(V - E_k\right) \end{cases} \quad (3)$$

where presynaptic LIF neuron model is stimulated only by an external stimulus current and adaptation current represented as $I_{applied}$ and I_a, respectively.

Postsynaptic current for LIF neuron shown by I_{Post} which includes astrocytic glutamate release, hydrolysis of ATP, excitatory synaptic, and adaptation currents that have been illustrated by I_{Glu}, I_{ATP}, and I_e, respectively. In synaptic and adaptation currents, g_e represents the value of excitatory conductance, E_e and E_k are the excitatory reversal potential the reversal potential of potassium. γ and η are the coupling coefficients for the variable G_m and the variable G_a, respectively.

B. ASTROCYTE MODEL

The neurotransmitter release (ATP, GABA, Glutamate) forms the synaptic cleft can trigger the secondary mediator IP3 production in the glial cells which leads the elevation levels of Ca2+ concentration. This elevation of Ca2+ oscillation can result in activation of postsynaptic neurons. The interaction model between the coupled neurons and astrocyte can be governed by the following nonlinear differential equations which describes the Ca2+ dynamics between extracellular space and cytoplasm [14], [15]:

$$\begin{cases} \tau_c\frac{dc}{dt} = -c - c_4 f\left(c, c_e\right) + r + \beta.S_m + \alpha w \\ \varepsilon_c\tau_c\frac{dc_e}{dt} = f\left(c, c_e\right) \\ \tau_{S_m}\frac{dS_m}{dt} = [1 + tanh\left(s_{S_m}(z - h_{S_m})\right)](1 - S_m) - \frac{S_m}{d_{S_m}} \\ \tau_{G_m}\frac{dG_m}{dt} = [1 + tanh\left(s_{G_m}(c - h_{G_m})\right)](1 - G_m) - \frac{G_m}{d_{G_m}} \\ \tau_{G_a}\frac{dG_a}{dt} = [1 + tanh\left(s_{G_a}(c - h_{G_a})\right)](1 - G_a) - \frac{G_a}{d_{G_a}} \end{cases} \quad (4)$$

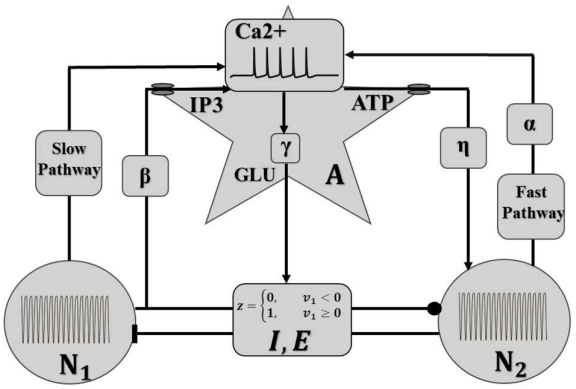

FIGURE 1. The general architecture for the functional pathways of the neuron-glial ensemble (tripartite synapse model) with considering the fast (shown by α), and slow (shown by β) activation pathways of the glial cells. Astrocyte response is controlled using η and γ which are called controlling parameters. Fast route can cause depolarization of glial cells and slow pathway is involved in IP3 production [14].

where c and c_e are the astrocytic calcium concentration in cytoplasm and calcium concentration in endoplasmic reticulum, respectively. $f(c, c_e)$ is used to describe the dynamic behavior of Ca2+ between cytoplasm and the endoplasmic reticulum, and gliotransmitters, G_m and G_a present astrocytic glutamate release and ATP production, respectively. The secondary messenger production is shown by variable S_m and controlled by element of β which can be activated by synaptic terminal. r, c_4, and ε_c represent the transmembrane current, constant for variable c, and the time separation constant. The component of αw defines the potassium activation pathway. The threshold values in the listed equations are named as h_{S_m}, h_{G_m}, and h_{G_a} used for activation and inactivation states of variable z and c, respectively. τ_c, τ_{S_m}, τ_{G_m}, and τ_{G_a} are used to show the controlling time scale for the existing variables. The controlling parameter of deactivation rates for each variable are shown by d_{S_m}, d_{G_m}, and d_{G_a}. The controlling parameter of steepness of activation for each variable are shown by s_{S_m}, s_{G_m}, and s_{G_a}. Variable z belongs to the synapse model. The complete structure for the tripartite synapse model which contains the main elements involved in the slow activation pathway is depicted in Fig. 1. The K activation pathway term has not been considered for the total calcium flux architecture. Parameter values that are employed for the simulation process are listed as Table. 1.

C. SYNAPSE MODEL

In this network, the functions $z_i(t)$ and $z_e(t)$ are used to define the time evolution of the inhibitory and excitatory currents between presynaptic and postsynaptic neurons, respectively which have been governed by the following equations [12]:

$$\begin{cases} \frac{dz_i}{dt} = T_i\left(1 - z_i\right) - \frac{z_i}{\tau_i} \\ \frac{dz_e}{dt} = T_e\left(1 - z_e\right) - \frac{z_e}{\tau_e} \\ T_i = 2\left[1 + tanh\ \frac{V_{Pre}}{4}\right] \\ T_e = 2\left[1 + tanh\ \frac{V_{Post}}{4}\right] \end{cases} \quad (5)$$

TABLE 1. The parameter values and controlling coefficients of the tripartite synapse models [14].

$c_1 = 0.13$	$c_2 = 0.9$	$c_3 = 0.004$	$c_4 = 50$
$\tau_c = 8$	$\tau_{S_m} = 100$	$\tau_{G_m} = 100$	$s_{S_m} = 100$
$h_{S_m} = 0.45$	$h_{G_m} = 0.5$	$d_{S_m} = 3$	$d_{G_m} = 3$
$h_s = -68$	$I_{applied} = 14$	$\tau_s = 10$	$k_s = 10$
$d_{G_a} = 3$	$h_{G_a} = 0.5$	$s_{G_a} = 100$	$\tau_{G_a} = 150$
$\varepsilon_c = 0.04$	$s_{G_m} = 100$	$S_s = 0.04$	$d_s = 3$

where $\tau_e = 2$ ms and $\tau_i = 10$ ms which are the time delay for the inhibitory and excitatory neurons.

D. STOCHASTIC COMPUTING

Stochastic computing paradigm is a digital realization approach which is presented in the 1960s [24]. This architecture purposes an extremely low-power and error-tolerant implementation which utilizes digital logics to perform arithmetic operations such as addition, division, and multiplication and relies on using binary bit-streams [24], [32]. In this approach, a sequence of random bit-streams is used to encode the real values which are interpreted as the probability of being either 1 or 0. For instance, the multiplication operation in stochastic computing representation can be performed using AND gate for unipolar format in the range of [0,1] and XNOR logic gate for bipolar format in the range of $[-1,1]$ which has been illustrated in Fig. 2. This approach has been employed in many applications to lower the computational complexity such as image and signal processing related problems, decoding of low-density parity-check (LDPC), and neural networks and bio-inspired approaches [33], [34], [35]. A stochastic computing system is composed of 3 main phases [25]: 1. Randomizer or stochastic number generator is used to convert binary bitstream to stochastic bitstream, 2. The main stochastic circuit design, and 3. De-randomizer is used to convert stochastic bitstream to binary bitstream which can be designed by using a counter. A general schematic diagram for this methodology is depicted in Fig. 3 [36].

IV. MODIFIED MODELS

In this section, the tripartite synapse model is modified based on the stochastic computing method to lower the hardware implementation cost and improve the computational efficiency. To achieve to this aim, the stochastic integrator is defined to solve the neural ordinary differential equations which can be designed using a stochastic number generator (SNG), and an n-bit up/down counter [24]. The stochastic integrator requires an n-bit up/down counter which works according to the initial values stored in the counter, and a stochastic number generator which includes a random number generator and a comparator, is required to encode the accumulated values in the counter [37]. To lower the hardware area and power consumption, the shared random number generators can be employed. The two-bit streams of a and b for the inputs of A and B can be considered for the up/down counter, respectively. The structure of the up/down counter

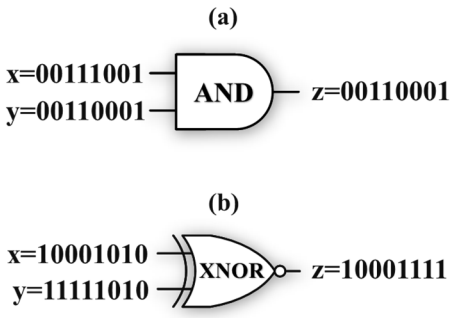

FIGURE 2. Basic stochastic computing elements representation, (a) Unipolar format of stochastic multiplier $P(xy = 1) = P(x = 1)P(y = 1) = xy$, (b) Bipolar format of stochastic multiplier $(2P(x = 1)-1)(2P(y = 1)-1) = xy$.

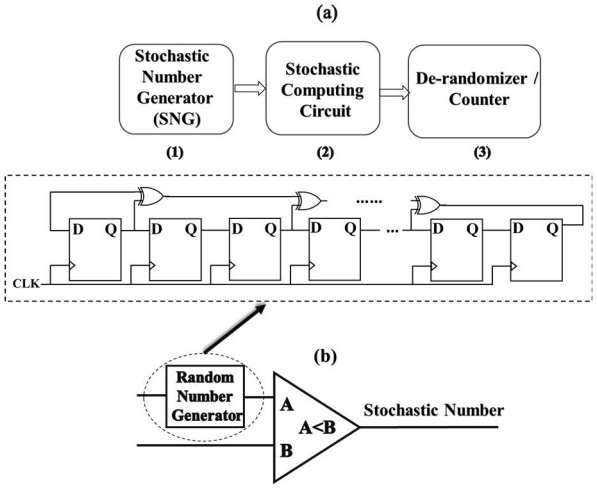

FIGURE 3. (a) a general structure for stochastic computing-based designs through (1) to (3), (b) stochastic number generator by illustrating the linear feedback shift register [36].

can be defined as:

$$I_{i+1} = \begin{cases} I_{i+1} & if\ a = 1\ and\ b = 0 \\ I_i & if\ a = b \\ I_{i-1} & if\ a = 0\ and\ b = 1 \end{cases} \quad (6)$$

where I_{i+1} and I_i represent the values that is saved in the counter at two clock cycles of $i + 1$ and i, respectively. a and b represent the value for both bit-streams of A and B, respectively. Therefore, ordinary differential equations (ODEs) can be approximated using the stochastic integrator based on the Euler method with step size of $1/2^n$ [38]:

$$\frac{dy(t)}{dt} = f(t, y(t)) \quad (7)$$

$$\frac{dy(t)}{dt} = \lim_{\Delta \to 0} \frac{y(t_i + \Delta t) - y(t_i)}{\Delta t} \approx \frac{y(t_i + h) - y(t_i)}{h} \quad (8)$$

$$\hat{y}_{i+1} = y_i + hf(t_i, y_i) \quad (9)$$

where h is the step size, Δt is the time interval and by considering $t_{i+1} = t_i + h$ based on the Euler's approach; therefor, $\hat{y}_{i+1}$ is the numerical simulation for function of $y(t)$ at t_{i+1},

i.e., $y(t_{i+1})$ which is shown in equation (9) [39]. Moreover, the probability of a and b at time t are presented by $p_a(t)$ and $p_b(t)$; thus, the numerical simulation of ODE can be estimated as:

$$\hat{y}_{i+1} = y_i + \frac{1}{2^n}\left[p_a\left(\frac{i}{2^n}\right) - p_b\left(\frac{i}{2^n}\right)\right]$$
$$\frac{dy(t)}{dt} = f(t, y(t)) = p_a(t) - p_b(t) \quad (10)$$

The stochastic integrator has been used for solving differential equation of Ca2+ dynamics and its corresponding variables in astrocyte and the membrane potential dynamics of LIF neuron model and the initial values of ODEs are set as the initial values of counter. Therefore, the postsynaptic neuron model with considering its different phases can be rewritten based on stochastic modes as follow:

$$V_{post}(t) = \begin{cases} V_{post}(t-1) + I_{post} \\ V_{post}(t) - E_L \\ if\ V_{post}(t) > V_{thr}\ \ then\ spiking \\ if\ V_{post}(t) = V_{thr}\ then\ rst \end{cases} \quad (11)$$

$$w_{post}(t) = \begin{cases} w_{post}(t-1) \\ if\ w_{post}(t) = w_{post}(t) + \delta\ then\ rst \end{cases} \quad (12)$$

where V_{thr} is the threshold value for the membrane voltage and δ is the incremental adaptation with each spike. When the postsynaptic current arrives, the synaptic integration phase starts, and the spike trains will be generated if the membrane voltage is greater than the threshold value. In the absence of the external currents, the neuron model experiences the leak integration phase. Thus, a stochastic mode of either 0 or 1 can be determined for each phase.

The existing variables in astrocyte model are required for the modification based on stochastic mode. Here, c_e which shows the Ca2+ concentration in ER, has a fast dynamic. Therefore, the equations belong to the original model can be modified by the following equations when $f(c, c_e) = 0$ [14], [15]. The nullcline of synapse model can be considered to approximate the z variable. The same concept can be applied for the glutamate release (G_m variable), the release of ATP (G_a variable), and the IP3 production (S_m variable) according to their corresponding threshold values. Consequently, the implementation cost of this simplified structure will be lowered in comparison to the original model. The results of this modification for both astrocyte and synapse models are described as follows:

$$\tau_c \frac{dc}{dt} = -c + (r + \beta S_m + \alpha w_{post}) \quad (13)$$

$$\frac{dz}{dt} = 0 \Rightarrow z = \frac{1 + tanh\ V_{Post}}{1 + \tau + tanh\ V_{Post}} = \begin{cases} 0, & V_{Post} < 0 \\ 1, & V_{Post} \geq 0 \end{cases} \quad (14)$$

$$S_m = \begin{cases} 0, & z < h_{S_m} \\ 1, & z \geq h_{S_m} \end{cases} \quad (15)$$

$$G_m = \begin{cases} 0, & c < h_{G_m} \\ 1, & c \geq h_{G_m} \end{cases} \quad (16)$$

$$G_a = \begin{cases} 0, & c < h_{G_a} \\ 1, & c \geq h_{G_a} \end{cases} \quad (17)$$

These functions can be implemented using stochastic binary projection as follows [40]:

$$x_b = \begin{cases} 1, with\ probability & p = \sigma(x) \\ 0, with\ probability & 1 - p \end{cases} \quad (18)$$

where, x_b is the binarized variable and p is the probability illustration of the synaptic transmissions, membrane voltage, and the corresponding variables of the astroglial model. In this expression, $\sigma(x)$ has been presented by the following expression:

$$\sigma(x) = max\left(0, min\left(1, \frac{x+1}{2}\right)\right) \quad (19)$$

V. HARDWARE DESIGN

In this section, a hardware implementation is presented for the proposed neuron and astrocyte models which includes the stochastic integrators, Stochastic Number Generators (SNG), and XNOR gates. In this design, the spiking neuron models and the glutamate-induced IP3 production in the glial cells with the astrocytic and synaptic currents are considered as the probabilistic-based models and illustrate the same behavior of the stochastic integrators. The hardware architecture for the proposed neuroglial interaction model with considering the synaptic connection is illustrated as Fig. 4 (A through C). For instance, the spiking neuron model fires when the membrane voltage reaches to its threshold value, similarly the stochastic integrators work based on the stored initial vales in the counter.

For the SNG unit, an n bit-LFSR (Linear Feedback Shift Register) is used to generate an uncorrelated and pseudo random sequence from 0 to 2^{n-1}. In this paper, an LFSR is shared between two SNGs with two comparators to reduce the occupied hardware overhead and create a low-correlated SNG circuit [41]. The shared-LFSR structure may result low accuracy of the design; therefore, a bit-rotation scheme can assist to reduce the cross-correlation between SNGs. In order to have a higher correlation in the output of the generated stochastic numbers, a l-bit randomly shifter used at the end of the LFSR to feed each SNGs. This structure has been employed for 6-bit and 8-bit LFSRs and illustrated in Fig. 5 [41]. According to this design, a tradeoff between the computational complexity, latency and time has been considered.

A basic block diagram which is used to explain the whole biochemical processes between the elements by considering the influence of coupling coefficients which exist within the neuroglial network has been depicted as Fig. 6.

VI. NEUROGLIAL NETWORK

In this section, the influence of astrocyte on the functionality of neuroglial network, has been investigated to realize

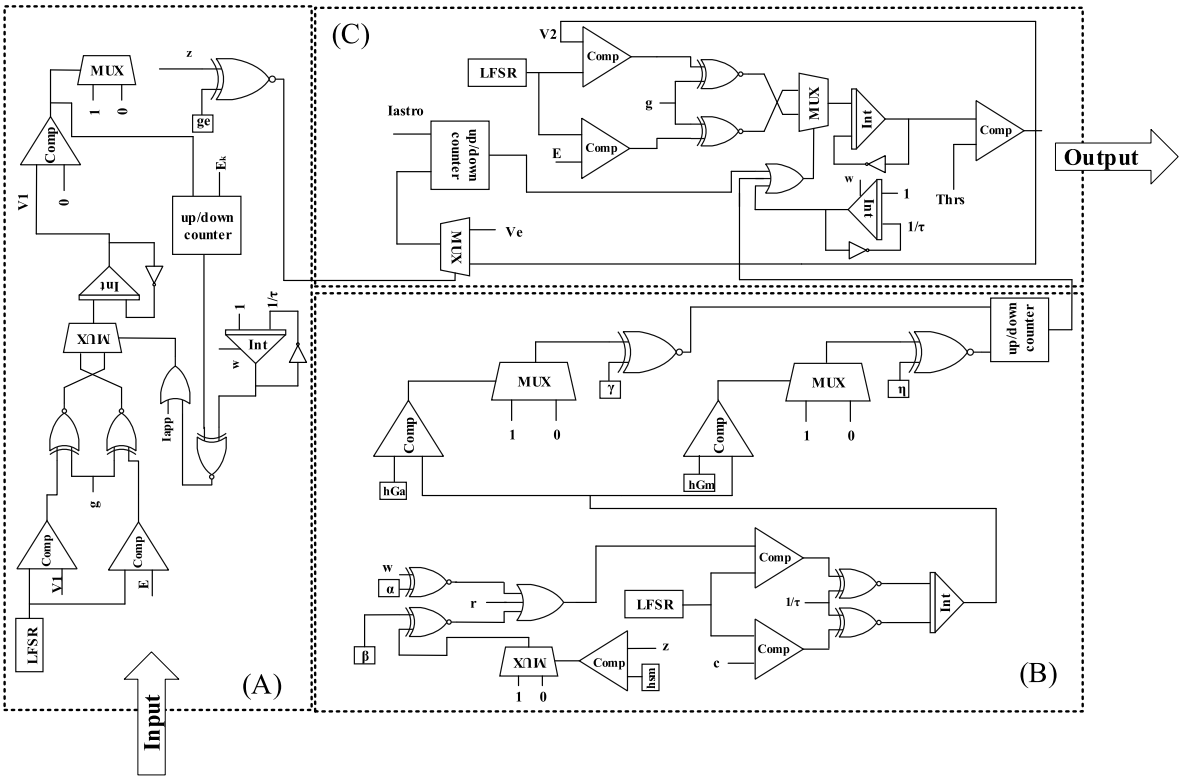

FIGURE 4. The proposed system architecture for membrane potential of presynaptic and postsynaptic LIF neuron, synaptic transmission between neurons, and cytosolic calcium in astrocyte models. (A) astrocyte model, (B) presynaptic neuron. (C) postsynaptic neuron.

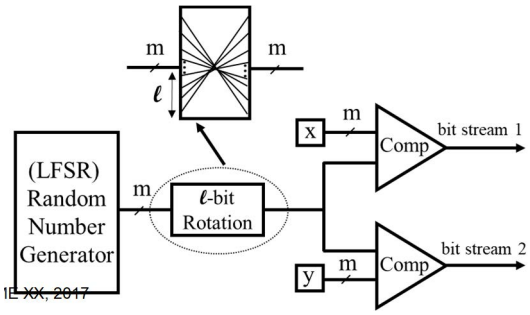

FIGURE 5. A shared LFSR between two SNGs.

its bidirectional communication with neurons for regulating the neuronal activities and desynchronization of the synchronized neurons for stabilizing the neuronal network behavior. Any disruptions within the functionality of glial cells can lead to a neurodegenerative disorder including the neuronal hyperexcitability and unpredictable epileptic seizures. Astrocytes are involved in the synaptic formation and are coupled to each other via gap junctions (GJs) which can provide a pathway for ions hemostasis and gliotransmitter release such as ATP and Glutamate. The schematic diagram for the neuroglial network and the interaction between its members which includes coupled neurons, synapses, and astrocytes is illustrated as Fig. 7(A). This architecture illustrates the essential influence of glial cells in desynchronization of the hyper-synchronized neurons.

A simple network according to the slow and fast activation pathway for various spiking patterns of a tripartite synapse is presented in Fig. 7 (B), that includes four astrocytes that are connected to their neighboring cells via gap junctions to form the astrocytic network. This network is called astroglia syncytium and a pair of coupled neurons is interacting with an astrocyte.

Thus, gap junction flow for IP3 ($JIP3$) and calcium (JCa^{2+}) between two neighboring cells through GJs, are governed by the following equations respectively [31], [42]:

$$J_{IP3i} = G_{IP3}\left([IP3]_i - [IP3]_k\right) \tag{20}$$

$$J_{Ca2+i} = G_c([c]_i - [c]_k) \tag{21}$$

where the IP3 gradient between two neighboring astrocytes is presented by $([IP3]_i - [IP3]_k)$, the flow of calcium in the network of cells can be shown by $([c]_i - [c]_k)$. G_{IP3} and G_c are the maximal flux diffusion (coupling strength) between two astrocytes through gap junctions for IP3 and Ca2+, respectively. According to these equations, i presents glial cell in the astroglial network and is situated to its adjacent cells that is specified by k. The astrocytic current which is shown by I_{astro} can be added to each neuron in tripartite synapse model also is defined as follow [1], [2]:

$$I_{astro} = \lambda_i [c], \quad i = 1, 2 \tag{22}$$

where λ_i is the coupling parameter for depolarizing currents from astrocyte to pyramidal neuron and interneuron. Calcium

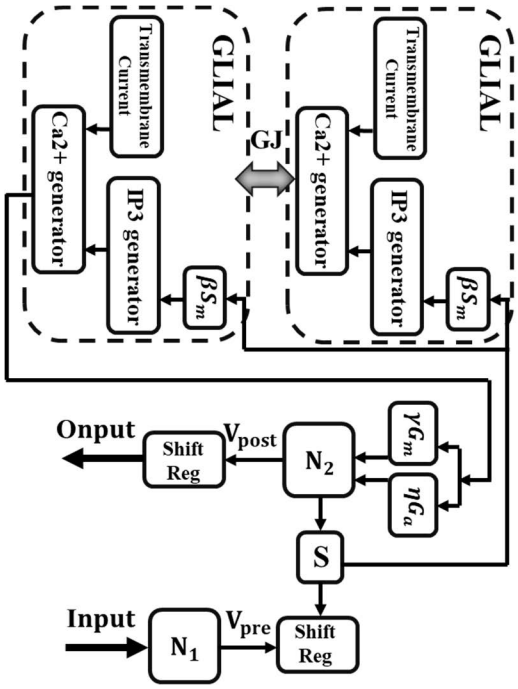

FIGURE 6. A basic diagram for the biochemical pathway and corresponding coupling coefficients in neuroglial network.

signalling can have an influence on the synaptic transmission from presynaptic to postsynaptic neuron through coefficient of λ_1 and λ_2.

IP3 is known as the second messenger. IP3 and calcium waves which can propagate through GJs from one astrocyte to the adjacent astrocyte are involved in the release of ATP and Glutamate within extracellular space. The gap junction coupling deficiency between glial cells in the network can lead to neuronal hyperexcitability which induces abnormal and periodic seizures. The coupling strength depends on the number of the gap junction coupling in astroglia network [43].

To evaluate the physiological and pathological situation of the glial cells, a measuring concept for the synchronization of neurons has been used by the following Kuramoto order parameter $\Re$ [44], [45]:

$$\Re(t)\, e^{i\Theta(t)} = \frac{1}{N_{osc}} \sum_{j=1}^{N} e^{i\varphi_j(t)} \tag{23}$$

where $\Theta(t)$ sets the mean phase, $\Re(t)$ is used to measure the synchronization index, N_{osc} measures the number of cells in the simulation, and $\varphi_j(t)$ is the phase of neuron j at time t that has been defined as [1]:

$$\varphi_j(t) = 2\pi \frac{t - t_n}{t_{n+1} - t_n} \tag{24}$$

where $t \in [t_n, t_{n+1}]$ and firing pattern can be included between this timing interval, t_n sets the onset time of the kth burst of jth neuron and is considered as $0 \leq \Re(t) \leq 1$ for all the time. When $\Re = 0$, oscillations are desynchronized, and for $\Re = 1$ phase synchronization will occur. A similar method for desynchronization of two coupled oscillators in [2] has also been employed for the simulation process of the modified and original models which is demonstrated in Fig. 8 (A through E). In this paper, gap junction coupling strength between astrocytes and applied current are also considered as the controlling parameters during the neuronal desynchrony and synchrony analysis. By increasing applied current, coupled neurons start interacting and becoming synchronized due to an elevation of the excitatory coupling coefficient on postsynaptic neuron. The other controlling parameters which are used for the simulation process, are listed as follows: GJ coupling coefficient ($G = 0$ and 1.4) and the rest of the parameters $\lambda_1 = 0.06$, $\lambda_2 = 0.11$, and $g_e = 0.02$. According to the results shown in Fig. 8, by changing the strength of GJ coupling, the mode of coupled neurons will fluctuate from in-phase to anti-phase synchronization mode and the impact of astrocytic syncytium can be examined on synchronized neurons. With strengthened coupling coefficient, anti-phase spiking rates can be observed.

The elevation of calcium ions in astrocyte and diffusion of Ca2+ waves and IP3 molecules via gap junctions in glial syncytium can assist in regulating the synaptic transmission between neurons over long distances. Therefore, the strength of astrocytic coupling can improve the spread of calcium signalling among astrocytic syncytium and respond to the neuronal activities. According to tripartite synapse model, gliotransmitter release such as ATP and Glutamate using coupling coefficients (shown by γ, η) can control the excessive excitatory current on postsynaptic neurons. In order to investigate the role of astrocytic syncytium in coordinating the synaptic plasticity, different values of coupling coefficients for tripartite synapse model (γ, η) and also maximal flux diffusion have been considered for analyzing the behavior of postsynaptic activity. The absence of astrocyte between presynaptic and postsynaptic neurons can be depicted in Fig. 9. An applied constant current will generate the action potential in presynaptic neurons which results a rise in excitatory synaptic conductance and activation of postsynaptic current on interneurons. In this case, the spiking rates of postsynaptic neurons uncontrollably will enhance, where the postsynaptic current cannot be regulated properly, and this can cause the pathophysiological conditions for the brain. The gap junction coupling strength between glial cells, astrocytic current due to glutamate release which causes depolarization of postsynaptic neuron and, the excitatory current on postsynaptic neuron can be modulated properly and this can prevent from unwanted neuronal hypersynchrony. The influence of the astrocytes between coupled neurons has been illustrated as Fig. 10. According to the results which have been shown in this figure, by increasing γ and η (Glutamate and ATP effects) and decreasing the GJ coefficient the rate of spiking activities among neurons also can alter and switch to epileptic conditions [46]. Therefore, the presence of astroglia network can prevent from excess extracellular potassium concentration and glutamate accumulation. This abnormal amount of potassium and glutamate can be eliminated by strong gap junctions coupling between astrocytes [47]. In this work,

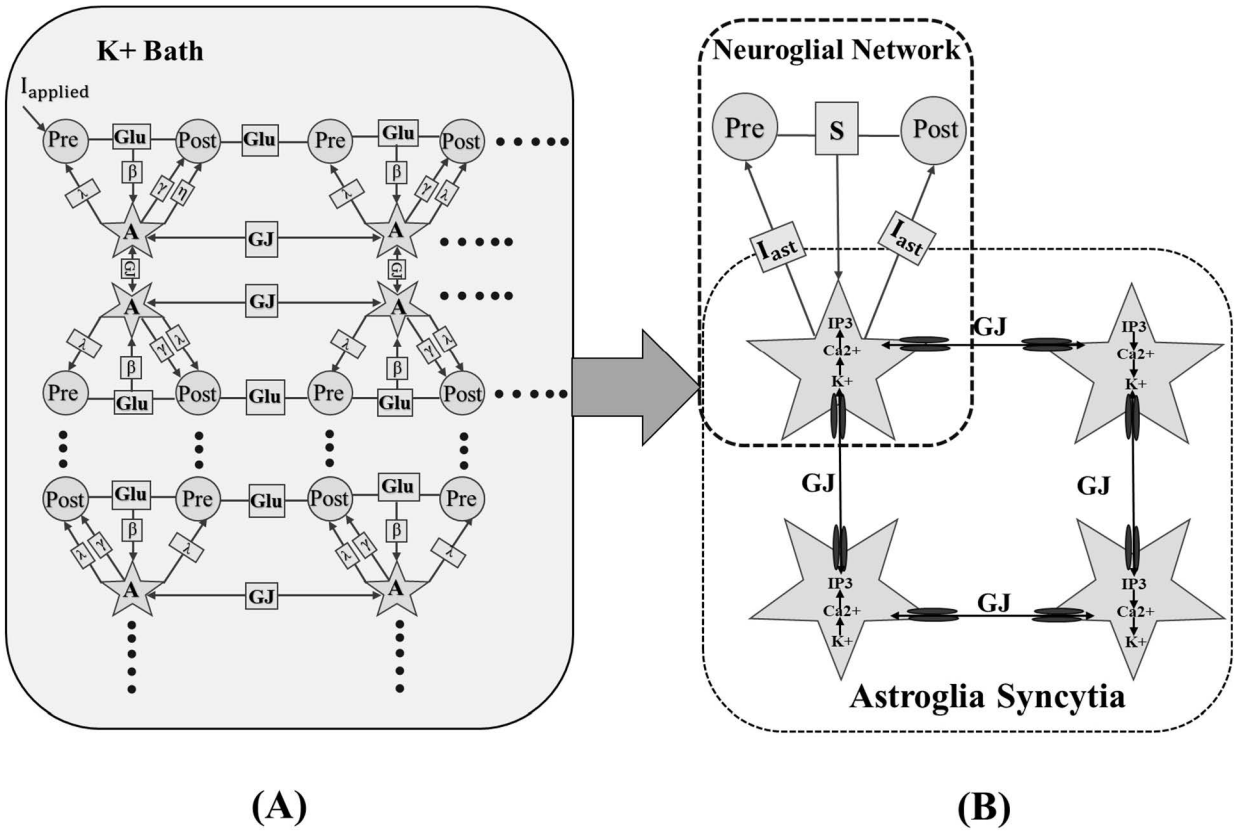

FIGURE 7. An architecture for neuro-glial behavior in hippocampus region of the brain. (A) A network of connected neurons through synaptic coupling, interacting with astrocytes. (B) coupled glial cells via gap junctions forming astroglia syncytium.

astrocytes are connected in a squared shape. Gap junction in astrocytic syncytium can redistribute the potassium (K+) ion and regulate neuronal activity. Uptake of glutamate and K+ can prevent from neurotoxicity. The balance of extracellular Potassium-glial concentration equation can be written as the following equation:

$$W\frac{d[K]}{dt} = \frac{1}{F}\sum_{i=1}^{N} I_{i,K} + G\left([K]_O - [K]\right) \tag{25}$$

where W is the measure of average distance between the glial cells, F is the Faraday's constant, $I_{i,K}$ shows the electrical current of potassium, and finally $G([K]_O - [K])$ is the diffusion of the potassium. G can be used as the controlling parameters for describing the neuronal synchrony between the coupled neuron [48]. The concentration of potassium in bath is shown by $[K]_O$.

The model of astrocyte can be extended as below for the glial network with considering coupled gap junctions:

$$\tau\frac{dc}{dt} = -c + r + \beta \cdot S_m + \sum_{i=1}^{n}\alpha_i w_i + \sum_{j=1}^{m} G_C\,[c]_j - [c] \tag{26}$$

where i is the number of neurons and j is the number of astrocytic cells which are existing in the neuroglial network. Different behavior of neuronal spiking activities using frequency spectrum (as Fast Fourier Transform and their corresponding histograms) are observed in [50]. On the other hand, FFT approach is used on the spiking activity of the coupled neurons according to increasing or decreasing coupling coefficients within the astroglia network. The results of this analysis for the original and the modified model have been demonstrated in Fig. 11. By selecting the appropriate coupling coefficients, the impact of astroglia network (as a regulator) in desynchronizing the hypersynchronous neurons has been evaluated. Synaptic coupling strength between neurons can activate potassium (K+) current after neuronal depolarization; therefore, this fast activation pathway can be controlled by parameter α (potassium activation pathway). In [49], the slow activation pathway in tripartite synapse and its impact on long term potentiation (LTP) of the postsynaptic spiking activity has been investigated to realize the closed loop behavior of neuroglial interaction model. In this paper, the impact of short-term potentiation (STP) mechanism is also considered on postsynaptic neurons which can be evaluated for adaptation (potassium) currents. By controlling parameter of α, extracellular K+ ions and STP can be regulated. The fast activation pathway causes glial cells depolarization due to rise of extracellular K+, and slow activation pathway activates astrocytes by IP3 production

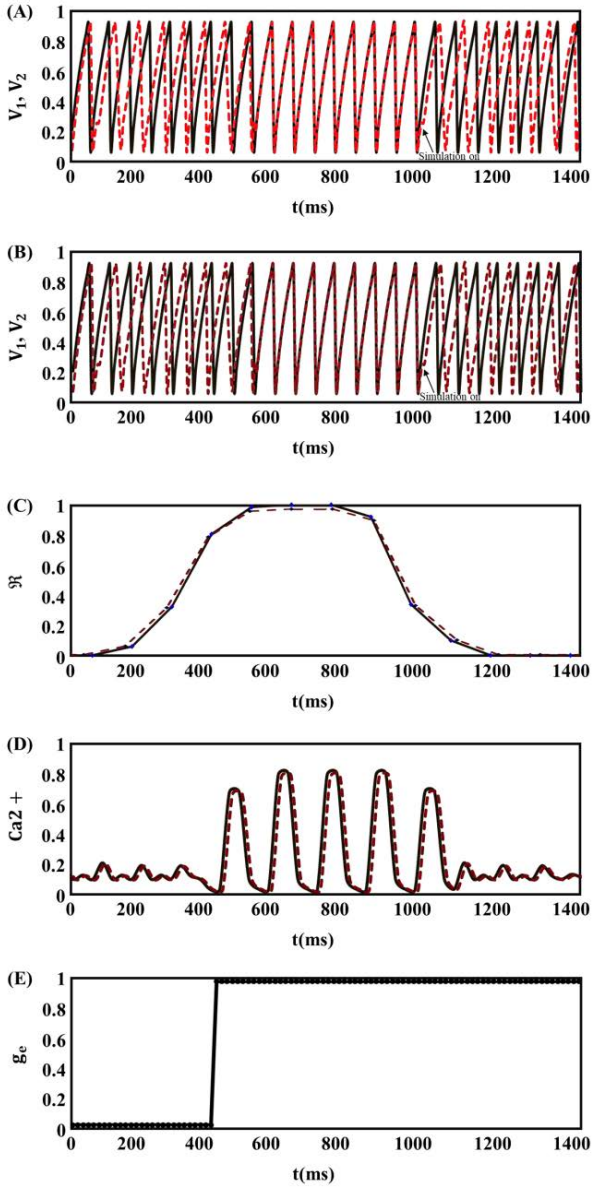

FIGURE 8. Effect of varying gap junction coupling strength between glial cells and the influence of astrocyte between two neurons during synchrony and desynchrony conditions for the original and proposed models. (A) membrane voltage for two coupled neurons by considering the role of the original astrocyte model (B) spike trains (membrane voltage) for two coupled neurons by considering the role of the modified astrocyte model. (C) Synchronization index for the original astrocyte model (black) and for the proposed astrocyte model (red). (D) (the output of original (black) and the modified (red) astrocyte model). (E) the effect of gap junction coupling between glial cells.

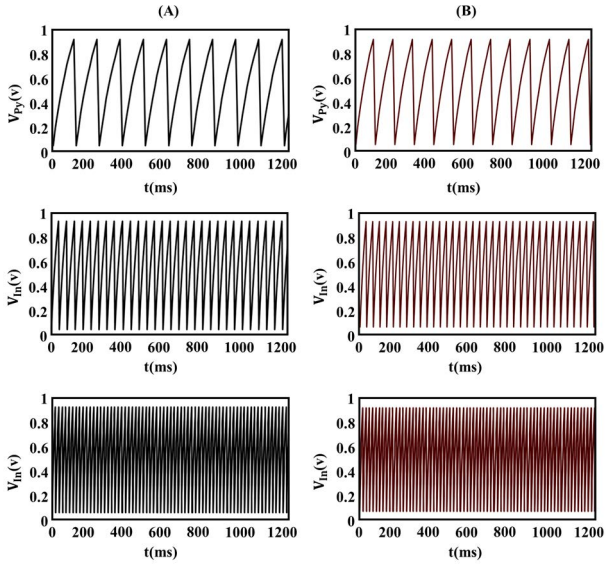

FIGURE 9. Membrane potential for the presynaptic and postsynaptic neurons without considering the influence of astrocytic network and its corresponding coupling coefficients. By increasing the excitation current on postsynaptic neuron, the frequency of the spiking activity has been enhanced. This can lead to the hyperexcitability of the neurons. (A) Spiking activity of presynaptic and postsynaptic neuron for the original model. (B) spiking activity of presynaptic and postsynaptic neurons for the modified model.

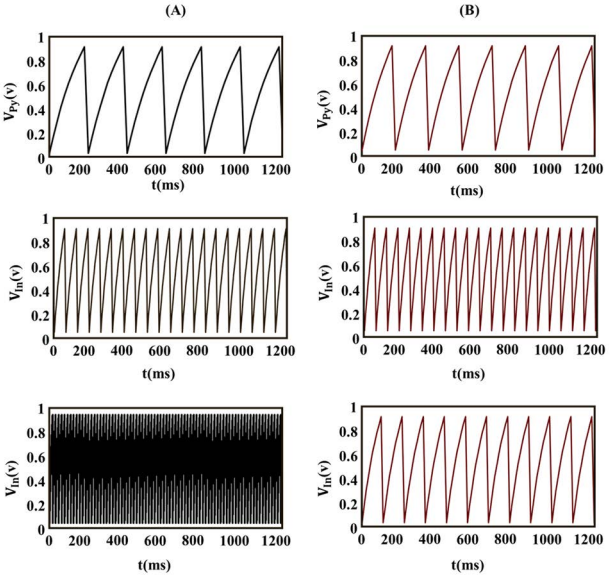

FIGURE 10. Influence of astroglial network on the spiking activity of postsynaptic neuron for the original and the modified models. In this case, by considering the neuron-astrocytic coupling coefficients, γ, η, and gap junction coupling between glial cells, the spiking activity of the postsynaptic neurons can be regulated and controlled. (A) Spiking activity (membrane potential) for the original model. (B) Spiking activity (membrane potential) for the modified model.

through synaptic strength. Fig. 12 illustrates that the firing rates unexpectedly can increase due to the rise of extracellular K+ ions when the gap junction rate between astrocytes is less than 0.4. Therefore, by controlling coupling parameters of the neuroglial interaction model, the frequency of firing rates can be managed.

In order to investigate the accuracy between the proposed model and the original biological neuroglial interaction models, Root Mean Square Error (*RMSE*) is computed and defined as follow:

$$RMSE\left(V_{org}, V_{modified}\right) = \sqrt{\frac{\sum_{i=1}^{n}\left(V_{org} - V_{modified}\right)^2}{n}} \tag{27}$$

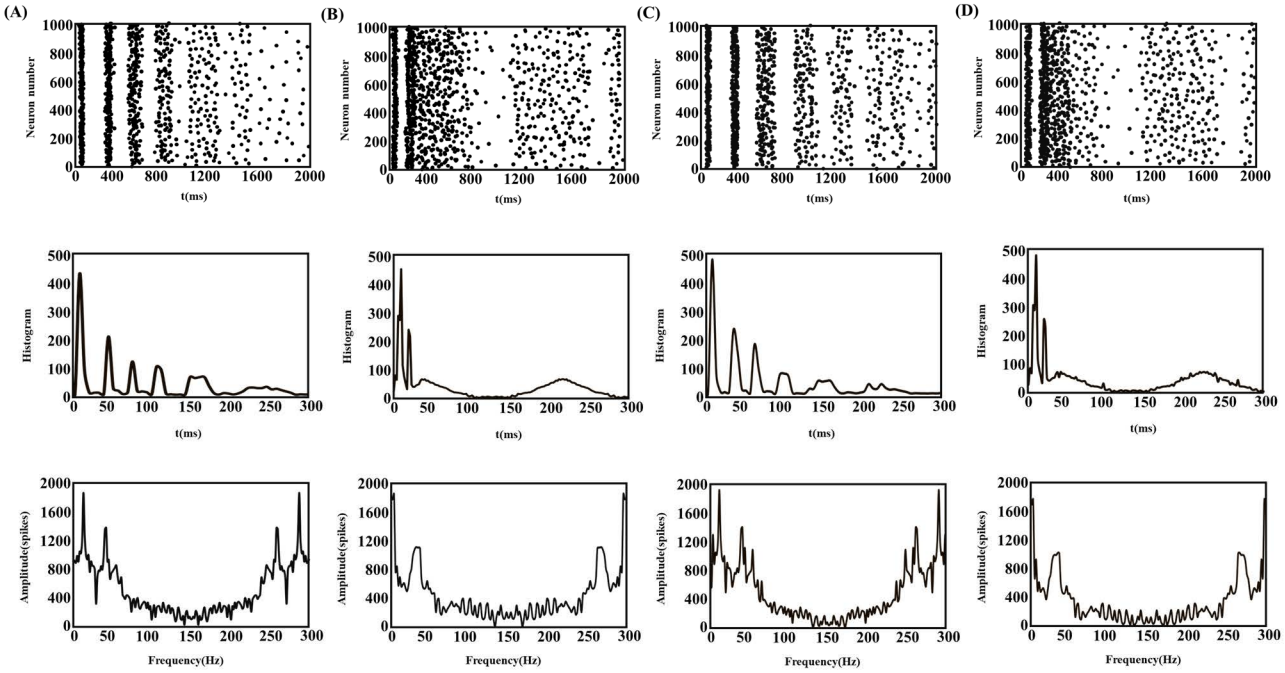

FIGURE 11. The effects of astrocyte in desynchronization of neurons firing. Raster plot representing the spiking activity neurons astrocytes (each neuron is randomly connected to other neurons through synapses and astrocytes), histograms for each state, and Fast Fourier Transform (FFT) for corresponding histograms. (A) spiking activity of neurons without considering the influence of astroglial syncytium for the original model. (B) spiking activity of neurons with considering the influence of astroglial syncytium in desynchronizing neurons for the original model. (C) spiking activity of neurons without considering the influence of astroglial syncytium for the modified model. (D) spiking activity of neurons with considering the influence of astroglial syncytium in desynchronizing neurons for the modified model.

TABLE 2. RMSE calculations for the neural spiking patterns using different time steps.

$I_{applied}$ (μA)	RMSE	NRMSE(%) $dt = 1/2^6$	RMSE	NRMSE(%) $dt = 1/2^8$
1.50	1.316	2.465	0.674	1.238
2.50	2.537	3.013	0.898	1.411
3.50	3.791	4.986	1.806	2.032
4.50	5.106	6.008	2.930	3.001

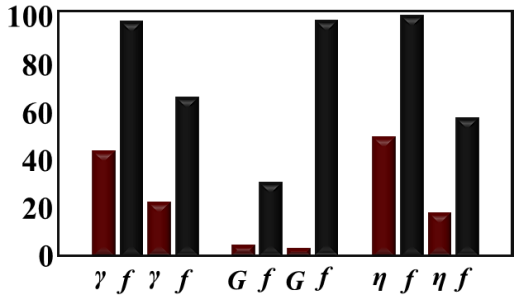

FIGURE 12. Demonstration of firing rates based on various coupling coefficients. Increment of parameters γ and η, can result in increasing spiking rates and by adjusting these two parameters spiking rates can be controlled. Strong gap junction coupling between astrocytes can regulate spiking rates; however, reduced gap junction strength cannot maintain spike rates.

where V_{org} and $V_{modified}$ represent the original values for the corresponding function and the modified values based on the

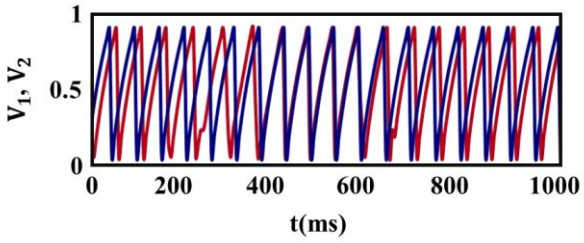

FIGURE 13. The output two coupled neurons by considering the impact of astrocytic syncytium.

SC-based values, respectively. The data length for the error measurement is shown by n. The Normalized Root Mean Square Error (NRMSE) can be obtained by the following equation:

$$NRMSE = \frac{RMSE}{V_{max} - V_{min}} \tag{28}$$

where V_{max} and V_{min} are the maximum and minimum values of membrane voltage.

The *RMSE* and *NRMSE* values according to the different excitation currents under various time steps are calculated and reported as Table. 2.

VII. IMPLEMENTATION RESULTS

This part presents the results of the hardware design for a neuroglial interaction model. As a proof of concept, the

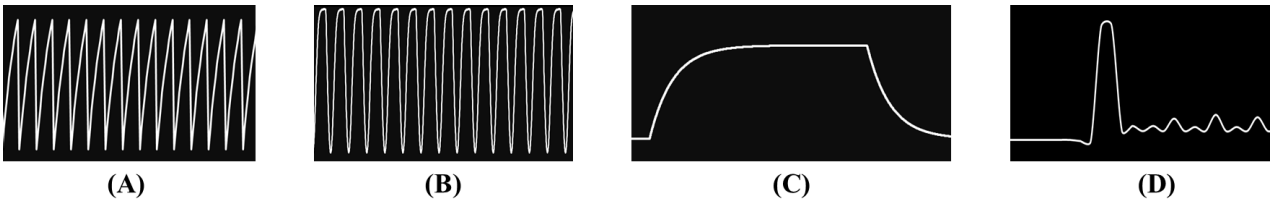

FIGURE 14. Digital oscilloscope captures of the modified model implemented on FPGA. (A) membrane voltage for LIF neuron model (tonic spiking). (B) membrane voltage for LIF neuron model (adaptation) (C) Secondary mediator (S_m), IP3 production. (D) Calcium spiking activity of the slow activation pathway with considering $\beta = 0.004$.

TABLE 3. Low level device utilization and the used percentage of the elements of the modified astrocyte and neuron models for the fast activation pathway.

Logic Utilization	Modified Neuron Model	Modified Astrocyte Model	Original Neuron Model	Original Astrocyte Model
Number of Slices	96	185	112	217
Number of LUTs	122	251	238	341
DSPs	0	0	1	7
Number of GCLKs	2	2	2	2

TABLE 4. Hardware resources comparison between the proposed model in this work and the previously published works.

Resources	Modified Models (N/A)	Model in [17] (N/A)	Model in [27] (N/A)	Model in [43] (N/A)	Model in [50] (N/A)	Model in [51] (N/A)	Model in [52] (N/A)
Registers	(96/185)	(−/3647)	(214/−)	(10383/11666)	(385/145)	(−/1065)	(35/262)
LUTs	(122/251)	(−/5813)	(140/−)	(9865/11394)	(441/273)	(−/1928)	(180/3052)
DSPs	(0/0)	(−/−)	(0/0)	(45/42)	(0/0)	(−/−)	(−/−)
Frequency (MHz)	192.53	251.196	–	–	–	139MHz	–

*(N/A) presents the results of hardware resources for Neuron and Astrocyte, respectively.

proposed circuit and the original models have been implemented on a XILINX Virtex-7 platform using ISE tools in order to evaluate the hardware performance. The output of the coupled neurons by considering the effect of glial cell on neuronal regulation is depicted in Fig. 13. Fig. 14. demonstrates the digital oscilloscope photographs of the proposed model for the membranate potential, calcium signalling, and IP3 production in astrocyte model which is implemented on the FPGA board. Low level device utilization details of the implemented original and the proposed models for the slow pathway activation mode have been summarized in Table. 3. The hardware analysis of the proposed astrocyte model in desynchronizing the hypersynchronous coupled neurons and regulating the synaptic transmission between presynaptic and postsynaptic neurons has the same performance of the original model. The power consumption analysis of the modified model is achieved by 138 mW in comparison to the original model which is realized by 316 mW.

The comparison results of the hardware realization in terms of the number of resources and maximum speed have been performed between the modified models and the previous proposed tripartite synapse models in [17], [27], [43], [50], [51], and [52]. These results are reported in Table. 4. In our proposed design, DSP block which is an expensive resource has not been employed within the implementation in comparison to the design which is proposed in [43]; therefore, the proposed architecture can provide less hardware complexity rather to the original models and the previously published research works. In [27], a hardware implementation using stochastic approach on the tripartite synapse is performed for 16-bit and 12-bit LFSRs; however, the detail of hardware resources for the astrocyte model has not been included in their work. The hardware resources of the neuron model have not been provided in [17] and the number of resources which is reported for the astrocyte model are greater than the hardware resources that are presented in this work. Additionally, 9 multipliers are used for the modified astrocyte in [17]. A digital implementation for a neuron-astrocyte model is proposed in [51]; however, the device resources are not summarized for the neuron model and the number of resources for the astrocyte model is greater than the proposed astrocyte model in this research article. Furthermore, the frequency of the design in [51] is reported 139MHz. A neuromorphic

TABLE 5. Hardware resources comparison between the proposed astrocyte model in this work and the recently published works for astrocyte models.

Resources	This work	Design in [53]	Design in [54]
Registers	185	670	675
LUTs	251	1345	1290
DSPs	0	4	8
BRAM	0	4	–

digital design for neuroglial interaction model by employing the linear approximation method is realized in [52]. Based on their research work, 5 multipliers are reported in the high-level utilization table.

A hardware cost comparison has been performed between the proposed astrocyte model in this work and two recently published articles according to different calcium-based astrocytic models in [53] and [54]. A digital design for an astrocyte model is implemented on FPGA platform which uses four DSP blocks and four block RAMs [53]. In [54], a set of piecewise linear approximation is presented for an astrocytic-based calcium signalling with the maximum speed of 81MHz. The result of this comparison is summarized in Table 5.

VIII. CONCLUSION

In this paper, a hardware implementation according to stochastic computing method for the neuron-glial interaction (tripartite synaptic model) based on the spiking neuron model and the Postnov astrocyte model [14], [15] has been presented. The impact of glial syncytium and its bidirectional communication between neurons and astrocytes for desynchronizing the abnormal and paroxysmal synchronized neurons within epileptic seizures in the neural network by considering appropriate coupling parameters is also investigated. The comparison results for the hardware and software implementation between the original biological models and the proposed models illustrate that the proposed models have lower hardware costs. The hardware implementation results of the proposed model are compared with previously published studies. The main aim of this study is to investigate the influence of astroglial network on different level of neural hyperexcitability during epileptic seizures. This work illustrates that the proposed design can be a good candidate for large scale bio-inspired neuroglial network hardware implementations on FPGA platforms.

REFERENCES

[1] M. Amiri, N. Hosseinmardi, F. Bahrami, and M. Janahmadi, "Astrocyte-neuron interaction as a mechanism responsible for generation of neural synchrony: A study based on modeling and experiments," *J. Comput. Neurosci.*, vol. 34, no. 3, pp. 489–504, Jun. 2013.

[2] G. Montaseri, M. J. Yazdanpanah, and M. Amiri, "Astrocyte-inspired controller design for desynchronization of two coupled limit-cycle oscillators," in *Proc. 3rd World Congr. Nature Biologically Inspired Comput.*, Oct. 2011, pp. 195–200.

[3] M. T. Barros, W. Silva, and C. D. M. Regis, "The multi-scale impact of the Alzheimer's disease on the topology diversity of astrocytes molecular communications nanonetworks," *IEEE Access*, vol. 6, pp. 78904–78917, 2018.

[4] S. Yang, J. Wang, N. Zhang, B. Deng, Y. Pang, and M. R. Azghadi, "CerebelluMorphic: Large-scale neuromorphic model and architectur for supervised motor learning," *IEEE Trans. Neural Netw. Learn. Syst.*, vol. 33, no. 9, pp. 4398–4412, Sep. 2022.

[5] E. Jokar, H. Abolfathi, A. Ahmadi, and M. Ahmadi, "An efficient uniform-segmented neuron model for large-scale neuromorphic circuit design: Simulation and FPGA synthesis results," *IEEE Trans. Circuits Syst. I, Reg. Papers*, vol. 66, no. 6, pp. 2336–2349, Jun. 2019.

[6] A. Basu, S. Ramakrishnan, C. Petre, S. Koziol, S. Brink, and P. E. Hasler, "Neural dynamics in reconfigurable silicon," *IEEE Trans. Biomed. Circuits Syst.*, vol. 4, no. 5, pp. 311–319, Oct. 2010.

[7] S. S. Woo, J. Kim, and R. Sarpeshkar, "A cytomorphic chip for quantitative modeling of fundamental bio-molecular circuits," *IEEE Trans. Biomed. Circuits Syst.*, vol. 9, no. 4, pp. 527–542, Aug. 2015.

[8] M. Hayati, M. Nouri, S. Haghiri, and D. Abbott, "Digital multiplierless realization of two coupled biological Morris-lecar neuron model," *IEEE Trans. Circuits Syst. I, Reg. Papers*, vol. 62, no. 7, pp. 1805–1814, Jul. 2015.

[9] A. Vetkas, J. Germann, G. Elias, A. Loh, A. Boutet, K. Yamamoto, C. Sarica, N. Samuel, V. Milano, A. Fomenko, B. Santyr, J. Tasserie, D. Gwun, H. H. Jung, T. Valiante, G. M. Ibrahim, R. Wennberg, S. K. Kalia, and A. M. Lozano, "Identifying the neural network for neuromodulation in epilepsy through connectomics and graphs," *Brain Commun.*, vol. 4, no. 3, Apr. 2022, Art. no. fcac092.

[10] L. S. Kumari and A. Z. Kouzani, "Electrophysiology-based closed loop optogenetic brain stimulation devices: Recent developments and future prospects," *IEEE Rev. Biomed. Eng.*, early access, Jan. 7, 2022, doi: 10.1109/RBME.2022.3141369.

[11] Z. Jia, Y. Lin, J. Wang, X. Ning, Y. He, R. Zhou, Y. Zhou, and L.-W. H. Lehman, "Multi-view spatial–temporal graph convolutional networks with domain generalization for sleep stage classification," *IEEE Trans. Neural Syst. Rehabil. Eng.*, vol. 29, pp. 1977–1986, 2021.

[12] A. D. Garbo, "Dynamics of a minimal neural model consisting of an astrocyte, a neuron, and an interneuron," *J. Biol. Phys.*, vol. 35, no. 4, pp. 361–382, Oct. 2009.

[13] S. Nadkarni and P. Jung, "Dressed neurons: Modeling neural–glial interactions," *Phys. Biol.*, vol. 1, no. 1, pp. 35–41, Mar. 2004.

[14] D. E. Postnov, L. S. Ryazanova, and O. V. Sosnovtseva, "Functional modeling of neural-glial interaction," *BioSystems*, vol. 89, no. 1, pp. 84–91, 2007.

[15] D. E. Postnov, R. N. Koreshkov, N. A. Brazhe, A. R. Brazhe, and O. V. Sosnovtseva, "Dynamical patterns of calcium signaling in a functional model of neuron-astrocyte networks," *J. Biol. Phys.*, vol. 35, no. 4, pp. 425–445, 2009.

[16] M. Heidarpur, P. Khosravifar, A. Ahmadi, and M. Ahmadi, "CORDIC-astrocyte: Tripartite glutamate-IP3-Ca^{2+} interaction dynamics on FPGA," *IEEE Trans. Biomed. Circuits Syst.*, vol. 14, no. 1, pp. 36–47, Feb. 2020.

[17] S. Haghiri, A. Ahmadi, and M. Saif, "VLSI implementable neuron-astrocyte control mechanism," *Neurocomputing*, vol. 214, pp. 280–296, Nov. 2016.

[18] H. Soleimani and E. M. Drakakis, "A compact synchronous cellular model of nonlinear calcium dynamics: Simulation and FPGA synthesis results," *IEEE Trans. Biomed. Circuits Syst.*, vol. 11, no. 3, pp. 703–713, Jun. 2017.

[19] H. Soleimani, M. Bavandpour, A. Ahmadi, and D. Abbott, "Digital implementation of a biological astrocyte model and its application," *IEEE Trans. Neural Netw.*, vol. 26, no. 1, pp. 127–139, Jan. 2015.

[20] S. Gomar, M. Mirhassani, M. Ahmadi, and M. Seif, "A digital neuromorphic circuit for neural-glial interaction," in *Proc. Int. Joint Conf. Neural Netw. (IJCNN)*, Jul. 2016, pp. 213–218.

[21] S. Haghiri, A. Naderi, B. Ghanbari, and A. Ahmadi, "High speed and low digital resources implementation of Hodgkin-Huxley neuronal model using base-2 functions," *IEEE Trans. Circuits Syst. I, Reg. Papers*, vol. 68, no. 1, pp. 275–287, Jan. 2021.

[22] S. M. Mohamed, W. S. Sayed, A. G. Radwan, and L. A. Said, "FPGA implementation of reconfigurable CORDIC algorithm and a memristive chaotic system with transcendental nonlinearities," *IEEE Trans. Circuits Syst. I, Reg. Papers*, vol. 69, no. 7, pp. 2885–2892, Jul. 2022.

[23] J. Cai, H. Bao, M. Chen, Q. Xu, and B. Bao, "Analog/digital multiplierless implementations for nullcline-characteristics-based piecewise linear Hindmarsh-Rose neuron model," *IEEE Trans. Circuits Syst., I, Reg. Papers.*, vol. 69, no. 7, pp. 2916–2927, Jul. 2022.

[24] B. R. Gaines, "Stochastic computing systems," in *Advances in Information Systems Science*, vol. 2, J. T. Tou, Ed. New York, NY, USA: Plenum, 1969, ch. 2, pp. 37–172.

[25] Z. Wang, D. Larso, M. Barker, S. Mohajer, and K. Bazargan, "Deterministic shuffling networks to implement stochastic circuits in parallel," *IEEE Trans. Very Large Scale Integr. (VLSI) Syst.*, vol. 28, no. 8, pp. 1821–1832, Aug. 2020.

[26] I. Polian, J. P. Hayes, V. T. Lee, and W. Qian, "Guest editors introduction: Stochastic computing for neuromorphic applications," *IEEE Des. Test*, vol. 38, no. 6, pp. 5–15, Dec. 2021.

[27] J. Liu, Z. Liang, Y. Luo, J. Huang, and S. Yang, "Hardware tripartite synapse architecture based on stochastic computing," in *Proc. Int. Symp. Theor. Aspects Softw. Eng. (TASE)*, vol. 1, Jul. 2019, pp. 81–85.

[28] V. Canals, A. Morro, A. Oliver, M. L. Alomar, and J. L. Rossellè, "A new stochastic computing methodology for efficient neural network implementation," *IEEE Trans. Neural Netw. Learn. Syst.*, vol. 27, no. 3, pp. 551–564, Mar. 2016.

[29] M. A. Hedayatpour, M. A. Karami, and J. Shamsi, "Implementation of Izhikevich neuron based on stochastic computing using a novel inspired Omega-Flip stochastic number generator," *Int. J. Circuit Theory Appl.*, vol. 50, no. 9, pp. 3104–3118, Sep. 2022.

[30] W. Gerstner and W. M. Kistler, *Spiking Neuron Models Single Neurons, Populations, Plasticity*. Cambridge, U.K.: Cambridge Univ. Press, Aug. 2002.

[31] J. Liu, J. Harkin, L. P. Maguire, L. J. McDaid, J. J. Wade, and G. Martin, "Scalable networks-on-chip interconnected architecture for astrocyte-neuron networks," *IEEE Trans. Circuits Syst. I, Reg. Papers*, vol. 63, no. 12, pp. 2290–2303, Dec. 2016.

[32] W. J. Poppelbaum, C. Afuso, and J. W. Esch, "Stochastic computing elements and systems," in *Proc. Fall Joint Comput. Conf. (AFIPS)*, Nov. 1967, pp. 635–644.

[33] A. Alaghi and J. P. Hayes, "Survey of stochastic computing," *ACM Trans. Embedded Comput. Syst.*, vol. 12, no. 2, pp. 1–19, May 2013.

[34] C. F. Frasser, P. Linares-Serrano, I. D. D. Los Rios, A. Moran, E. S. Skibinsky-Gitlin, J. Font-Rossello, V. Canals, M. Roca, T. Serrano-Gotarredona, and J. L. Rossello, "Fully parallel stochastic computing hardware implementation of convolutional neural networks for edge computing applications," *IEEE Trans. Neural Netw. Learn. Syst.*, early access, Apr. 22, 2022, doi: 10.1109/TNNLS.2022.3166799.

[35] T. Hirtzlin, B. Penkovsky, M. Bocquet, J.-O. Klein, J.-M. Portal, and D. Querlioz, "Stochastic computing for hardware implementation of binarized neural networks," *IEEE Access*, vol. 7, pp. 76394–76403, 2019.

[36] Y. Liu, S. Liu, Y. Wang, F. Lombardi, and J. Han, "A stochastic computational multi-layer perceptron with backward propagation," *IEEE Trans. Comput.*, vol. 67, no. 9, pp. 1273–1286, Sep. 2018.

[37] S. Liu and J. Han, "Hardware ODE solvers using stochastic circuits," in *Proc. 54th Annu. Design Autom. Conf.*, Jun. 2017, pp. 1–6.

[38] S. Xiao, W. Liu, Y. Guo, and Z. Yu, "Low-cost adaptive exponential integrate-and-fire neuron using stochastic computing," *IEEE Trans. Biomed. Circuits Syst.*, vol. 14, no. 5, pp. 942–950, Oct. 2020.

[39] J. C. Butcher, *The Numerical Analysis of Ordinary Differential Equations: Runge–Kutta and General Linear Methods*. Hoboken, NJ, USA: Wiley, Feb. 1987.

[40] I. Hubara, M. Courbariaux, D. Soudry, R. El-Yaniv, and Y. Bengio, "Binarized neural networks," in *Proc. 30th Conf. Neural Inf. Process. Syst.*, 2016, pp. 4107–4115.

[41] H. Ichihara, S. Ishii, D. Sunamori, T. Iwagaki, and T. Inoue, "Compact and accurate stochastic circuits with shared random number sources," in *Proc. IEEE 32nd Int. Conf. Comput. Design (ICCD)*, Oct. 2014, pp. 361–366.

[42] A. Moshkforoush, L. Balachandar, C. Moncion, K. A. Montejo, and J. Riera, "Unraveling ChR2-driven stochastic Ca^{2+} dynamics in astrocytes: A call for new interventional paradigms," *PLOS Comput. Biol.*, vol. 17, no. 2, Feb. 2021, Art. no. e1008648.

[43] J. Liu, J. Harkin, L. P. Maguire, L. J. McDaid, and J. J. Wade, "SPANNER: A self-repairing spiking neural network hardware architecture," *IEEE Trans. Neural Netw. Learn. Syst.*, vol. 29, no. 4, pp. 1287–1300, Apr. 2018.

[44] P. F. Pinsky and J. Rinzel, "Synchrony measures for biological neural networks," *Biol. Cybern.*, vol. 73, no. 2, pp. 129–137, Jan. 1995.

[45] N. Chakravarthy, S. Sabesan, L. Iasemidis, and K. Tsakalis, "Controlling synchronization in a neuron-level population model," *Int. J. Neural Syst.*, vol. 17, no. 2, pp. 123–138, Apr. 2007.

[46] D. Terman and M. Zhou, "Modeling the role of the astrocyte syncytium and K+ buffering in maintaining neuronal firing patterns," *Opera Medica Et Physiologica*, vol. 5, no. 1, pp. 7–16, Mar. 2019.

[47] R. K. Orkand, J. G. Nicholls, and S. W. Kuffler, "Effect of nerve impulses on the membrane potential of glial cells in the central nervous system of amphibia.," *J. Neurophysiology*, vol. 29, no. 4, pp. 788–806, Jul. 1966.

[48] D. E. Postnov, L. S. Ryazanova, and R. A. Zhirin, "Noise controlled synchronization in potassium coupled neural models," *Int. J. Neural Sys.*, vol. 17, no. 2, pp. 105–113, 2007.

[49] M. Hayati, M. Nouri, S. Haghiri, and D. Abbott, "A digital realization of astrocyte and neural glial interactions," *IEEE Trans. Biomed. Circuits Syst.*, vol. 10, no. 2, pp. 518–529, Apr. 2016.

[50] S. Haghiri, A. Ahmadi, and M. Saif, "Complete neuron-astrocyte interaction model: Digital multiplierless design and networking mechanism," *IEEE Trans. Biomed. Circuits Syst.*, vol. 11, no. 1, pp. 117–127, Feb. 2017.

[51] S. Nazari, K. Faez, M. Amiri, and E. Karami, "A novel digital implementation of neuron–astrocyte interactions," *J. Comput. Electron.*, vol. 14, no. 1, pp. 227–239, Mar. 2015.

[52] F. Faramarzi, F. Azad, M. Amiri, and B. Linares-Barranco, "A neuromorphic digital circuit for neuronal information encoding using astrocytic calcium oscillations," *Frontiers Neurosci.*, vol. 13, p. 998, Oct. 2019.

[53] M. Isik, A. Paul, M. L. Varshika, and A. Das, "A design methodology for fault-tolerant computing using astrocyte neural networks," in *Proc. 19th ACM Int. Conf. Comput. Frontiers*, May 2022, pp. 169–172.

[54] S. Haghiri and A. Ahmadi, "Digital FPGA implementation of spontaneous astrocyte signalling," *Int. J. Circuit Theory Appl.*, vol. 48, no. 6, pp. 1–15, Jan. 2020.

MAHSASADAT SEYEDBARHAGH is currently pursuing the Ph.D. degree in electrical and computer engineering with the University of Windsor, Windsor, ON, Canada.

Her research interests include digital implementation of bioinspired circuits and systems, neuroglial stimulation, and computational neuroscience.

ARASH AHMADI (Senior Member, IEEE) received the B.Sc. degree in electrical engineering from the Sharif University of Technology, in 1993, the M.Sc. degree in electronics engineering from Tarbiat Modares University, Tehran, Iran, in 1997, and the Ph.D. degree in electronics from the University of Southampton, U.K., in 2008. From 2008 to 2010, he was a Fellow Researcher with the SpiNNaker project at the University of Southampton. He was an Associate Professor with the Electrical Engineering Department, Razi University, from 2010 to 2014, and a Visiting Scholar at the University of Windsor, Canada, from 2014 to 2021. He is currently an Assistant Professor with the Electronic Department, Carleton University, Ottawa, Canada. His current research interests include domain-specific hardware design and optimization, neuromorphic, AI-on-a-chip, bio-inspired computing, and memristors.

MAJID AHMADI (Life Fellow, IEEE) received the B.Sc. degree in electrical engineering from the Sharif University of Technology, Tehran, Iran, in 1971, and the Ph.D. degree in electrical engineering from the Imperial College, London University, London, U.K., in 1977. Since 1980, he has been with the Department of Electrical and Computer Engineering, University of Windsor, Windsor, ON, Canada, where he is currently a Professor and the Director of the Research Center for Integrated Microsystems. He has coauthored the book *Digital Filtering in One-D and Two Dimensions: Design and Applications* (New York: Plennum, 1989) and has authored more than 500 articles in the areas of digital signal processing, pattern recognition and computer vision, neural network architectures and applications, VLSI circuits, and testing and computer arithmetic. His current research interests include digital signal processing, MEMS, machine vision, pattern recognition, traditional, and bioinspired neural network architectures, and VLSI implementation. He is a fellow of IET, U.K. He was a recipient of an Honorable Mention Award from the Editorial Board of the *Journal of Pattern Recognition*, in 1992, and the Distinctive Contributed Paper Award from the Multiple-Valued Logic Conference Technical Committee and the IEEE Computer Society, in 2000. He is currently an Associate Editor of the *Journal of Pattern Recognition* and served as a Regional Editor for the *Journal of Circuits, Systems and Computers*. He was the IEEE Circuits and Systems Society Representative on the Neural Network Council and the Chair of the IEEE Circuits and Systems Neural Systems Applications Technical Committee.